A Solution Conformation Analysis of Forocidins I and Isoforocidins I Using NMR and Molecular Modeling

Kumar Ramu,[1,2] Sachin Shringarpure,[1] and John S. Williamson[1,3]

Received August 3, 1994; accepted November 15, 1994

KEY WORDS: forocidin I; isoforocidin I; 16-membered macrolides; proton-NMR, carbon-NMR, two-dimensional spectra; HETCOR; COSY; modified Karplus equation; molecular modeling; X-ray; demycarosyl leucomycin A_3.

INTRODUCTION

Spiramycins, discovered in 1954, are 16-membered macrolides produced by *Streptomyces ambofaciens* (1). They show antimicrobial activity against *Toxoplasma gondii* and *Cryptosporidium*, protozoal opportunistic infections associated with AIDS (2,3). The correlation between chemical structure and biological activity of the family of 16-membered macrolides is limited but studies indicate that there is a loss of activity in spiramycins devoid of sugar moieties. The absolute stereochemical requirements and their effect on the activity of this series of compounds has yet to be investigated.

We have recently presented a complete NMR spectral characterization of the spiramycins I and III (4). Our current interests involve producing derivatives of the spiramycins employing techniques such as selective microbial biotransformations of spiramycin biosynthetic precursors such as the forocidins (acid hydrolytic products of spiramycin I) (Fig. 1). This endeavor has required a complete and explicit spectral characterization of both the spiramycins (4) as well as the forocidins.

The major objective of the present study was to determine the conformation of the forocidins in solution using molecular dynamics and two-dimensional NMR data. The dihedral angles and coupling constants have been estimated using extended Karplus-type equations, the results of which have been compared to those obtained from the X-ray data for 13-OH demycarosyl Leucomycin A_3 (4,5). With an understanding of the solution conformation of this spiramycin hydrolytic product, one may better deduce how the parent compound, spiramycin, as well as analogs of spiramycin affect biological activity. ^{1}H-NMR and ^{13}C-NMR assignments (Tables 1 and 2) of the forocidins I (6,7) (Figure 3) and the isoforocidins I (4,5) (Figure 4) are also reported here.

[1] Department of Medicinal Chemistry and the Research Institute of Pharmaceutical Sciences, School of Pharmacy, University of Mississippi, University, Massachusetts 38677.

[2] Department of Pharmacology and Toxicology, University of Texas at Austin, Texas 78712.

[3] To whom correspondence should be addressed.

MATERIALS AND METHODS

Although the spiramycins are marketed commercially (Sigma Chemical Co.) as a mixture of spiramycins I, II and III, we were not able to detect any significant amounts of spiramycin II in the mixture. Spiramycin I was easily separated from the commercial mixture of spiramycins using a modified column chromatography procedure and monitoring the column fractions by TLC (4). Thermospray LC/MS spectra were obtained in the column bypass mode using 50% methanol in 0.1 M ammonium acetate as the mobile phase and a Vestec Model mass spectrometer with a Technivent data system and thermospray interface which was attached to a Waters Associates 600-MS HPLC system. HPLC grade ammonium acetate, methanol (MeOH) and acetonitrile (ACN) were obtained from Fisher Scientific.

Hydrolysis of Spiramycin I

The spiramycins were hydrolyzed using a modified (6) procedure. Spiramycin I (1 g) was dissolved gradually in 3 ml of 1 N HCl and stirred on a magnetic stirrer for a period of 15 hr at room temperature. The hydrolysis reaction was monitored by TLC [2:1:1, $CHCl_3$:MeOH:10% NH_4OH (bottom layer) using UV [254 nm] and *p*-anisaldehyde spray reagent; spiramycin I {R_f = 0.8} and hydrolytic product {R_f = 0.2}]. After the completion of the reaction (spiramycin I totally consumed), the pH of the solution was adjusted to 9.0 using 1 M NaOH. This solution was extracted with ethyl acetate (3 × 100 ml) and the solvent evaporated to yield 0.45 gms of the hydrolytic product (forocidins and the cleaved sugars).

The forocidins (R_f = 0.2) were separated from the sugar residues (R_f = 0.4) using column chromatography [(9.5:0.5, 9.0:1.0, 8.5:1.5 in order of increasing polarity), $CHCl_3$:MeOH] and the column fractions were monitored by TLC [5:1, $CHCl_3$:MeOH using by *p*-anisaldehyde spray reagent]. The forocidin mixture (0.200 g), a white powder, was further dried in vacuum (24 hr). Thermospray LC/MS data of the forocidin mixture indicated a single peak for the pseudomolecular ion ($M + 1^+ = m/z$ 558).

HPLC Purification of Forocidins

The solvent system; 60:35:5, 0.1 M aq. ammonium acetate:MeOH:ACN was used as the mobile phase. Ammonium acetate (9.24 gms) was completely dissolved in distilled water (1200 ml), MeOH (700 ml) and ACN (100 ml) were added to make up 2000 ml of the mobile phase. The mobile phase was stirred on a magnetic stirrer for a period of 15 min until all phases were miscible, filtered through a 0.47 micron filter (Alltech) using a Supelco filtering apparatus connected to a water aspirator (20-25 torr) and degassed as per the instructions in the Shimadzu High Performance Liquid Chromatography instruction manual.

Using the elution solvent, the forocidins were purified by semi-preparative reversed phase HPLC on a C_{18} column (Alltech Econosil, 22.5 mm × 25 cm) with a Shimadzu LC 600 (500 µl loop attached to the Rheodyne injector 7161) solvent delivery system at 5 ml/min, coupled to a Shimadzu SP 6A spectrophotometric detector operating at a wave-

0724-8741/95/0400-0621$07.50/0

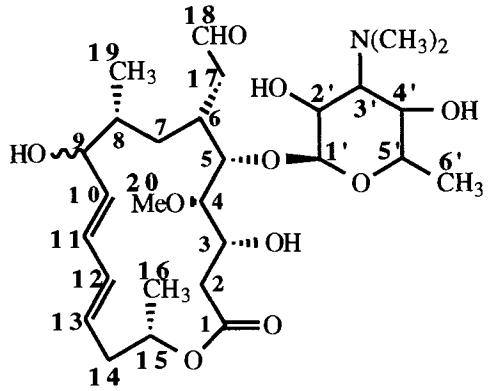

Fig. 1. Structure and numbering system used for Forocidins.

length of 232 nm. The data was analyzed by a Shimadzu Chromatopac CR 601 recorder. Five injections of the forocidin mixture (100 μl × 200 mg/ml each) were made. Two fractions, I (Retention time = 40 min) and II (Retention time = 80 min) corresponding to the two peaks in the UV chromatogram were collected separately and concentrated using a Buchi Rotavapor®. The remaining solution was adjusted to pH 9.0 using 1 N NaOH and extracted (5×) with chloroform. The chloroform extracts were pooled and the fractions lyophilized on the Savant Lyophilizer to yield fractions I (33 mg) and II (40 mg).

Further purification of fractions I and II was accomplished by column chromatography using $CHCl_3$:MeOH (9:1, 8.5:1.5, 8:2, in order of increasing polarity). The column fractions were monitored by TLC (5:1, $CHCl_3$:MeOH). Compounds IA (4) (25 mg, 25% yield, m.p. 197–199°C, Mol. wt. 557) and IB (5) (1 mg, 1% yield, Mol. wt. 557) were obtained from fraction I (Fig. 4) after evaporation of the column fractions. Similarly compounds IIA (6) (15 mg, 15% yield, m.p 143–146°C, Mol. wt. 557) and IIB (7) (10 mg, 10% yield, m.p. 143–146°C, Mol. wt. 557) were obtained from fraction II (Fig. 3). Thermospray LC/MS mass spectral data of each of the hydrolytic products indicated a single peak for the pseudomolecular ion ($M + 1^+ = m/z$ 558) and no fragment peaks were observed using this soft ionization technique.

NMR Spectral Characterization of the Forocidins

NMR spectra were obtained in $CDCl_3$ on a Varian VXR-300 spectrometer operating at 300 MHz for proton and at 75 MHz for carbon. All samples were dissolved separately in 0.5 ml of deuterated chloroform ($CDCl_3$) to obtain the 1-D proton, 1-D carbon, APT, DEPTGL, 2-D COSY (^1H-^1H correlation experiment) and 2-D HETCOR (^1H-^{13}C correlation experiment) phase-modulated spectra. The APT, DEPTGL (7), COSY (90°) (8) and HETCOR (9) experiments were performed using the standard Varian software (Tables 1 and 2).

The ^1H-NMR spectra was obtained with double precision using a spectral width of 4,100 Hz using 30 K data points, a 45° pulse angle, a 3.66 s acquisition time, a 2.0 s relaxation delay and a total of 16 transients. With double precision, data are obtained using a 32 bit integer format instead of the standard 16 bit format, thus enabling the acquisition of ^1H-NMR spectrum for 16 transients with a better signal to noise ratio. In the absence of double precision, acquisition of the ^1H-NMR spectrum (using 32 K data points and 3.996 s acquisition time) is automatically aborted after a maximum number of transients (5 repetitions) are obtained. The ^{13}C-NMR spectrum was obtained using a spectral width of 16,502 Hz using 32 K data points, a 45° pulse angle, a 0.9 s acquisition time, a 3.0 s relaxation delay, Waltz modulated proton decoupling and a total of 250 transients.

The COSY spectrum was obtained using a narrowed 2,358 Hz spectral width in both dimensions, a 90° acquisition pulse angle, a 0.217 s acquisition time, a 1.0 s relaxation delay, 256 increments each with 5 repetitions in the second frequency domain, pseudo-echo shaped data processing, giving a total acquisition time of 38.0 min. Double precision was not used for the COSY experiment and therefore the number of repetitions was set at 5 which is the maximum possible. The HETCOR spectrum was obtained using 9,785 Hz spectral width in the 1-D (F2-carbon) dimension and 2,358 Hz in the 2-D (F1-proton) dimension, a 90° acquisition pulse angle, a 0.105 s acquisition time, a 1.0 s relaxation delay, 64 increments each with 1000 repetitions in the second frequency domain, broadband modulated proton decoupling, pseudo-echo shaped data processing, giving a total acquisition time of 20 hours.

Molecular Modeling

The X-ray model for 13-OH demycarosyl Leucomycin A_3 (5) was built using MicroChem®. Molecular mechanics and energy minimization was accomplished using "CSC Chem 3D® Plus (version 3.0, Cambridge Scientific Computing)" software on the Macintosh-Plus™ to arrive at the structures for the forocidins and isoforocidins that were consistent with the NMR data. The twisting of the 16-membered lactone ring and conformation of the various substituents was determined from key dihedral angles and $^3J_{HH}$ coupling constants estimated (Tables 3 and 4) using an "Extended Karplus-type equation" (10,11) generated coupling table that takes into account the heteroatom substitution on the adjacent carbon atoms. The MM2 parameters used in the CSC Chem 3D® Plus software are a combination of those from Allinger's MM2 program, Ponder's TINKER system and the rest from Cambridge Scientific Computing, Inc. The default MM2 parameters were used.

RESULTS AND DISCUSSION

Acid Hydrolysis of Spiramycin I

A literature procedure (6) describing spiramycin I hydrolysis indicated the formation of a single product using 2 N HCl for a period of 15 hr at 37°C. On repeating this procedure, it was observed that the reaction was completed at, essentially, zero time (TLC indicated total conversion of spiramycin I). After a period of 15 hr the reaction yielded a black mixture, indicating acid decomposition of spiramycin at these conditions. When spiramycin I was hydrolyzed using 0.1 N HCl for 15 hr at 37°C (12) the hydrolysis process stopped with the formation of neospiramycin (4) (loss of the mycarose sugar from spiramycin), while further hydrolysis to forocidin (loss of mycarose and forosamine sugars from spiramycin) did not occur.

Table 1. ^{1}H-NMR Chemical Shift Assignments of Forocidins

Proton #	(6) 9α-OH F I	(7) 9β-OH F I	(4) 13α-OH ISF I	(5) 13β-OH ISF I
2a (2β)	2.66 dd	2.66 dd	2.64 dd	
	(11.0,16.0)	(11.0,16.0)	(11.1,16.0)	
2b (2α)	2.19 dd	2.19 dd	~2.17	
	(1.0,16.0)	(1.0,16.0)		
3	3.78 d	3.99 d	3.96 d	
	*11.0)	(11.0)	(11.1)	
4	3.07 d	3.05 d	3.11 d	
	(8.7)	(10.1)	(8.5)	
5	4.11	3.97	3.75 d	
	(10.1)NR	(10.1)NR	(8.5)	
6	~2.25	~2.15	~2.17	
7a	1.32(NR)	~1.35	~1.35	
	(13.5)			
7b	0.85 ddd	0.84	0.84	
	(1.9,8.1,13.5)	(7.0,14.1)NR	(7.3,13.9)NR	
8	1.90 m	~2.09	~2.17	~1.73
9	4.09	4.43	6.08 dd	6.11
	(9.7)NR	(4.3)NR	(10.6,15.5)	
10	5.67 dd	5.62 dd	5.99 dd	~5.92
	(9.7,15.3)	(4.3,15.3)	(9.4,15.5)	
11	6.25 dd	5.78 dd	6.12 dd	~6.61
	(10.5,15.3)	(9.1,15.3)	(9.4,15.6)	
12	6.01 dd	5.98 dd	5.54 dd	~5.62
	(10.5,15.3)	(9.1,15.4)	(8.6,15.6)	(8.2,15.3)
13	5.63 ddd	6.14 ddd	4.13 ddd	3.85 ddd
	(1.5,8.9,15.3)	(1.5,9.1,15.4)	(5.0,8.6,13.9)	(0.9,1.3,8.2)
14a (14β)	2.09 ddd	2.09 ddd	1.9 (2H)	
	(2.3,8.9,9.8)	(2.3,9.1,9.8)	(17.5)NR	
14b (14α)	1.85 ddd	1.85 ddd		
	(1.5,8.7,9.8)	(1.5,8.7,9.8)		
15	5.27 ddd	5.24 ddd	5.12 ddd	~5.02
	(2.3,6.6,8.7)	(2.3,6.4,8.7)	(0.6,6.3,12.2)	
16	1.29 d	1.25 d	1.23 d	
	(6.6)	(6.4)	(6.3)	
17a (17_{ax})	2.90 ddd	2.90 ddd	2.93 ddd	
	(1.5,9.5,17.7)	(1.5,9.5,17.7)	(1.1,9.5,17.9)	
17b (17_{eq})	2.42 dd	2.42 dd	2.37 dd	
	(3.6,17.7)	(3.6,17.7)	(3.5,17.9)	
18	9.80 s	9.77 s	9.76 s	9.74 s
19	1.02 d	1.02 d	1.02 d	1.00 d
	(6.6)	(6.8)	(6.8)	
20	3.50 s	3.52 s	3.53 s	3.47 s
1′	4.48 d	4.43	4.43 d	
	(7.2)	NR	(7.47)	
2′	3.52	3.55	~3.47	
	(8.2)	NR		
3′	2.78	2.78	2.53	
	NR	NR	(10.9)NR	
4′	3.5 dd	3.26 dd	~3.13	
	(8.9,9.5)	(9.0,10.7)		
5′	3.32 dq	3.36 dq	3.31 dd	
	(5.7,8.9)	(6.3,9.0)	(6.1,8.6)	
6′	1.20 d	1.20 d	1.26	
	(5.7)	(6.3)	(6.1)	
3′ $N(Me)_2$	2.62 s	2.77 s	2.61 s	2.56 s

* Values in parenthesis are the observed coupling constants in the 1D ^{1}H-NMR spectra.
~ indicates proton chemical shift from center of 2-D HETCOR experiment.
a,b indicate the methylene (CH_2) protons, 'a' being more downfield than 'b.'
NR indicates that the proton signal was either partially overlapped or unresolved.
s = singlet, d = doublet, t = triplet, dd = doublet of doublets, ddd = doublet of doublet of doublets, dq = double of quartets, m = multiplet.

Table 2. ^{13}C-NMR Chemical Shift Assignments of Forocidins

Carbon #		(6) 9α-OH F I	(7) 9β-OH F I	(4) 13α-OH ISF I	(5) 13β-OH ISF I
1	C=O	174.0	173.7	173.1	173.5
2	CH_2	33.8	38.9	38.6	37.6
3	CH–O	68.2	66.8	67.0	69.4
4	CH–O	85.0	85.4	85.8	85.3
5	CH–O	79.6	81.2	80.7	78.4
6	CH	29.7	31.5*	31.2*	29.5
7	CH_2	30.6	38.5	29.7	30.4
8	CH	31.0	32.8*	31.6*	33.2
9	CH–O	73.1	67.9	132.3	80.4
10	CH=	129.8	134.9	128.5	128.2
11	CH=	134.4	139.9	141.5	135.1
12	CH=	132.3	129.2	133.5	132.7
13	CH=	131.8	128.6	73.1	132.3
14	CH_2	37.8	41.4	42.7	41.1
15	CH–O	69.2	67.1	68.6	68.9
16	CH_3	20.1	21.6	21.7*	20.4
17	CH_2	43.1	46.1	45.7	42.9
18	C=O	202.6	202.3	202.5	202.9
19	CH_3	14.8	17.7	17.8	16.2
20	CH_3–O	61.7	61.6	61.7	62.1
1′	CH–O	104.2	104.1	104.3	104.5
2′	CH–OH	70.6	70.2	70.7	71.8
3′	CH–N	71.1	72.3	71.2	69.1
4′	CH–O	70.3	69.7	70.3	75.1
5′	CH–O	73.3	73.1	73.3	73.0
6′	CH_3	17.8	20.9	21.6*	19.1
3′	$N(Me)_2$	41.8	42.1	41.8	42.1

* May have interchangeable assignments.

The hydrolysis procedure was modified using 1 N HCl at 37°C. By comparing R_f values (product R_f 0.2, spiramycin I R_f 0.7) with those in the literature (6), the final hydrolytic product (forocidin I) was determined. Thermospray LC/MS data of the product showed a single peak corresponding to the pseudomolecular ion (M + 1 = m/z 558) of forocidin. In contrast to earlier reports (6), a 300 MHz ^{1}H-NMR analysis of the hydrolytic product indicated a mixture of compounds. Two aldehydic peaks were observed between 9–10 ppm along with duplicate peaks with respect to the rest of the molecule. Attempts to separate the compounds by recrystallisation from benzene, methanol, methanol-water proved unsuccessful. Purification of the hydrolytic products using preparative TLC also proved futile.

When leucomycin A_3 is hydrolyzed (Fig. 2) in 0.3 N HCl two macrolide products are formed, 9-OH forocidin II (9-OH demycarosyl leucomycin A_3) and 13-OH isoforocidin II (13-OH demycarosyl leucomycin A_3), due to an intramolecular allylic rearrangement, while hydrolysis in 0.1 N HCl forms only the 9-OH (13). Based on this information we predicted 9-OH forocidin I and 13-OH isoforocidin I as the two probable products formed during the hydrolysis reaction.

Purification of the Hydrolytic Products

Purification of the hydrolysis mixture was carried out by reversed phase HPLC on a C_{18} column pre-attached to a C_{18} reversed phase cartridge guard column. The chromatogram showed two peaks corresponding to two fractions, fraction I (Retention time = 40 min) and fraction II (Retention time = 80 min) which were separated. Interestingly, once again the ^{1}H-NMR spectrum (in deuterated $CDCl_3$) of both fractions I and II showed two aldehydic signals in the region between 9–10 ppm as well as a host of overlapping signals in the olefenic region. Careful evaluation of the ^{1}H-NMR spectra of each fraction indicated the presence of at least four compounds, two in each of the fractions eluted on HPLC. The entire chromatographic process was repeated using a semi-prep reversed phase C_{18} column where greater quantities of fractions I and II were collected. Further purification of fractions I and II using HPLC recycling and different solvent conditions was unsuccessful. Each of the fractions I and II were subjected to normal phase stepped-gradient column chromatography using silica gel with a mobile phase of chloroform and methanol. Compounds IA (4) and IB (5) were obtained from fraction I while compounds IIA (6) and IIB (7) were obtained from fraction II.

Molecular Modeling Studies

Structural analysis of the resulting forocidins and isoforocidins was substantiated using the X-ray data for 13-OH demycarosyl Leucomycin A_3 (isoforocidin II) (2), a close structural analog as a guide (6). Using (2) as the backbone, forocidins I (6,7) and the isoforocidins I (4,5) were built. Molecular mechanics energy minimization molecular modeling was used to arrive at the structures for the forocidins I (6,7) (Fig. 3) and isoforocidins I (4,5) that were consistent with the NMR data. The conformational results from molecular modeling and NMR data were compared to the X-ray

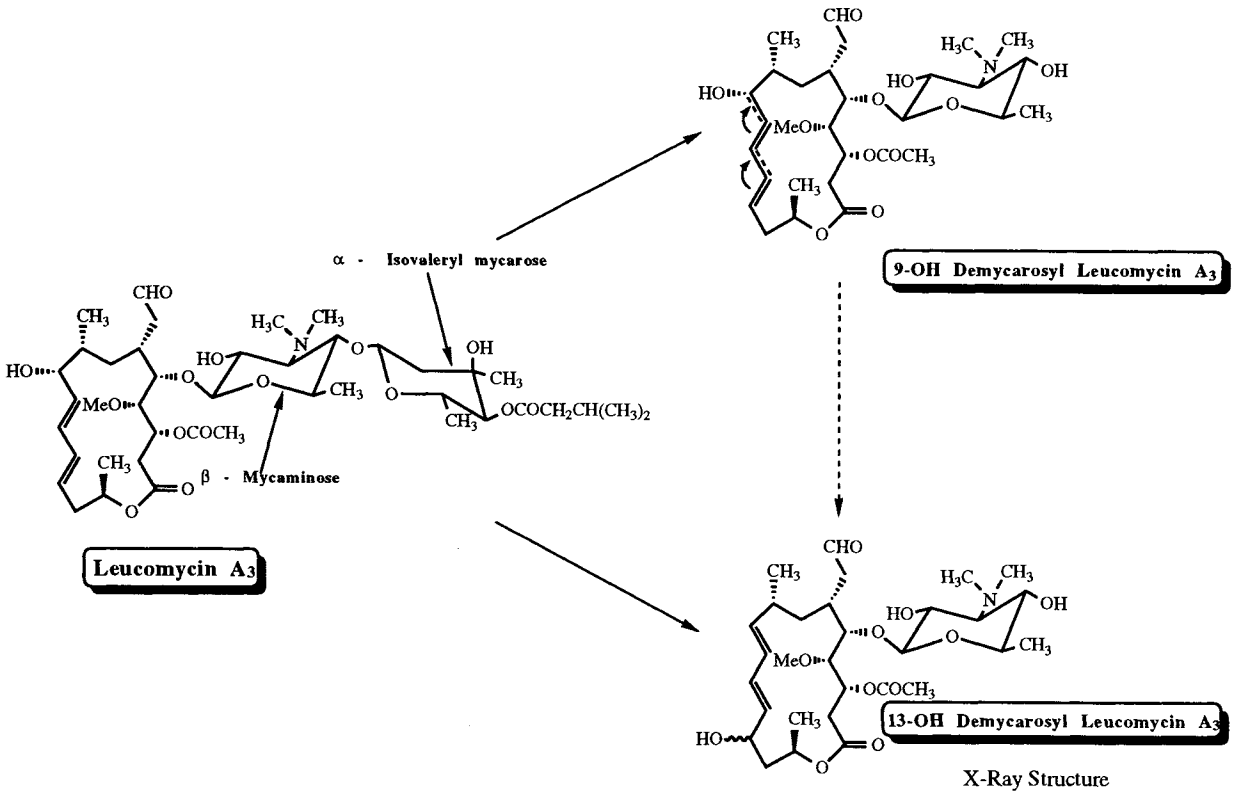

Fig. 2. Allylic rearrangement, hydrolysis of Leucomycin A_3.

data. The twisting of the 16-membered lactone ring and conformation of the various substituents were determined from key dihedral angles (Tables 3 and 4) and $^3J_{HH}$ coupling constants estimated using an extended Karplus-type equation that takes into account the heteroatom substitution on the adjacent carbon atoms. This equation is not suitable for olefinic protons.

Extended Karplus-type Equation ---

$$J = A + B\cos\theta + C\cos 2\theta + \cos\theta\,[(\Delta S1 + \Delta S4)\cos(\theta - 120) + (\Delta S2 + \Delta S3)\cos(\theta + 120)]$$

The Sugar Portion of the Compounds (4,5,6,7)

The sugar regions of all the compounds were similar. Of the three anomeric sugar protons H-1′, H-1″, and H-1‴ in spiramycin I, H-1′ is a doublet for the hydrolytic products and showed a strong cross-peak to the adjacent methine proton H-2′ in the 2D-COSY spectrum while protons H-1″ and H-1‴ were absent. This indicated the loss of both mycarose and forosamine sugars from spiramycin I and thereby the formation of forocidin I. From the cross-peaks in the 2D-HETCOR spectrum corresponding to H-1′, we identified the carbon signal C-1′ while C-1″ and C-1‴ signals of spiramycin I were absent. Also, the proton and carbon signals for the dimethyl amino group 4‴-NMe_2 of forosamine and 7″ methyl of mycarose were absent. This confirmed that spiramycin I was hydrolyzed with the loss of mycarose and forosamine sugars to forocidin I. The remainder of the mycaminose proton signals were determined with the help of the COSY spectrum. Proton H-2′ appeared as a doublet of doublets coupling into the methine H-3′ which in turn coupled to the adjacent proton H-4′. The proton H-4′ appeared as a doublet coupling into methine proton H-5′ which in turn coupled strongly to the methyl proton doublet H-6′. The cross-peaks in the HETCOR spectrum corresponding to the sugar protons helped identify the carbon signals C-2′, C-3′, C-4′, C-5′ and C-6′. The forocidins and isoforocidins have a basic amino sugar β-D-mycaminose, which has an α stereochemistry with the aglycone.

Forocidin I [compound IIA, (6)] (Fig. 3)

The ^{1}H-proton NMR spectrum of compound IIA (6) appeared similar to that of spiramycin I except for the loss of two sugars. The compound was identified as a 'forocidin I' analog since the hydroxyl group was at position C-9. The aldehydic carbon at ~200.0 δ was assigned to the aldehydic carbonyl C-18 since there was a cross-peak in the HETCOR spectrum to the broad singlet at ~9.6 δ which was assigned to the aldehydic proton H-18. A weak cross-peak between H-18 and the methylenes H-17a and H-17b (in the case of the methylene protons 'a' being designated to the signal more downfield and the other as 'b') indicated by the COSY spectrum explained the multiplicity (broad singlet) to the aldehydic proton. Both the methylene protons which appeared as multiplets show cross-peaks to C-17 in the HETCOR spectrum and to H-6 in the COSY spectrum. These cross-peaks helped to accurately locate the position of the methine proton H-6 and carbon C-6 from the COSY and HETCOR spectrums respectively. The methylene protons H-17a and H-17b

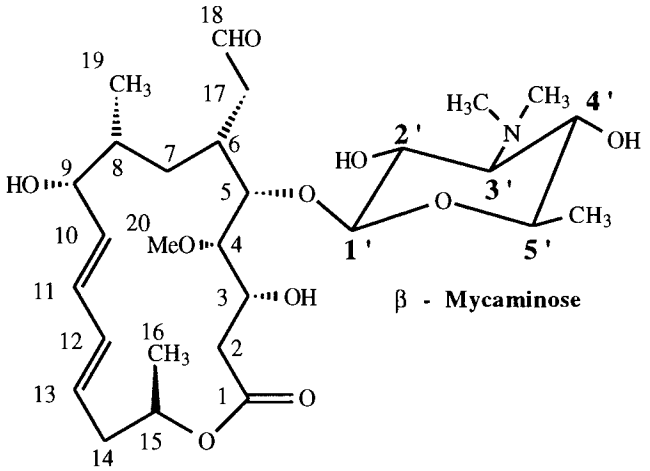

(6) Compound II A
9 α-OH Forocidin I

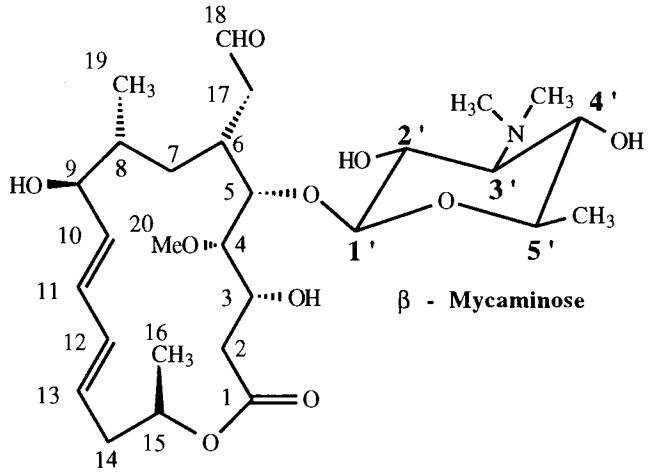

(7) Compound II B
9 β-OH Forocidin I

Fig. 3. Forocidins I.

not only showed geminal coupling (observed value for $J_{17a,17b}$ = 17.7 Hz), but also coupled very weakly to protons H-18 (observed values for $J_{17a,18}$ = 1.5 Hz, $J_{17b,18}$ = not resolved) and strongly to H-6 (observed values for $J_{17a,6}$ = 9.5 Hz, $J_{17b,6}$ = 3.6 Hz). Coupling constants for protons H-17 (axial) and H-17 (equitorial) were calculated from the dihedral angles obtained for the minimized structure of 9α-OH forocidin I (Table 4). The coupling of H-17_{eq} to H-6 was small ($J_{17eq,6}$ = 2.8 Hz) while that of H-17_{ax} to H-6 was large ($J_{17ax,6}$ = 14.7 Hz). The proton H-18 being on an sp2 carbon, Karplus equation cannot calculate the coupling constants between protons H-17 and H-18. The observed coupling constants for H-17 cross-checked agreeably with the observed values for H-6, while the appearance of H-18 as a broad singlet indicated that the coupling between H-18 and H-17 were negligible. Thus we can characterize H-17a (downfield) as H-17_{ax} and H-17b (upfield) as H-17_{eq} protons.

The downfield methine proton multiplet (~5.27 ppm) was assigned to H-15 which coupled to the methylenes H-14a and H-14b and strongly to the methyl doublet H-16. From their respective cross-peaks in the HETCOR spectrum, the carbons C-15 and C-16 were determined. The methylene protons H-14a and H-14b, which appeared as multiplets, showed cross-peaks in the COSY spectrum to the olefenic proton H-13, which was a doublet of doublets of doublets and cross-peaks to C-14 in the HETCOR spectrum thus differentiating between the methylene carbons C-14 and C-17 was straightforward. The methylene protons H-14a and H-14b besides coupling geminally (observed value for $J_{14a,14b}$ = 9.8 Hz), also coupled to protons H-13 (observed values for $J_{14a,13}$ = 8.9 Hz, $J_{14b,13}$ = 1.5 Hz) and H-15 (observed values for $J_{14a,15}$ = 2.3 Hz, $J_{14b,15}$ = 8.7 Hz). Coupling constants for protons 14α (axial) and 14β (equitorial) were calculated from the dihedral angles obtained for the minimized structure of 9α-OH forocidin I (Table 4). The coupling of H-14β to H-15 was small ($J_{14\beta,15}$ = 3.0 Hz) while that of H-14α to H-15 was large ($J_{14\alpha,15}$ = 13.9 Hz). The proton H-13 being olefinic, Karplus equation cannot calculate the coupling constants between protons H-14 and H-13. The observed coupling constants for H-14 cross-checked agreeably with the observed values for H-13 and H-15. Thus we can characterize H-14a as H-14β and H-14b as H-14α.

Table 3. Calculated Dihedral Angles and Coupling Constants for Isoforocidins I

	(4) 13α-OH ISF I		(5) 13β-OH ISF I	
Proton	Calculated Dihedral Angle	Calculated J_{H-H}	Calculated Dihedral Angle	Calculated J_{H-H}
2β-3	−172.485	12.92	−172.190	12.88
2α-3	70.315	0.97	70.667	0.95
3-4	−53.923	−0.15	−54.106	−0.16
4-5	−178.238	11.59	−179.553	11.60
5-6	−70.207	0.40	−70.752	0.38
6-7β	166.902	14.80	167.439	14.83
6-7α	−77.497	1.29	−77.023	1.32
6-17eq	−65.124	2.69	−64.933	2.72
6-17ax	177.135	14.75	177.315	14.75
7β-8	−59.770	3.15	−58.973	3.26
7α-8	−174.118	14.92	−173.230	14.91
8-9	−4.141	—	−2.027	—
8-19 CH_3	—	7.10	—	7.10
9-10	−179.684	—	−180.000	—
10-11	177.949	—	178.296	—
11-12	178.951	—	178.859	—
12-13	163.627	—	−79.974	—
13-14β	65.344	3.07	−54.033	2.65
13-14α	−179.000	13.55	60.933	0.03
14β-15	−66.315	1.71	−65.308	1.81
14α-15	177.925	14.10	179.553	14.13
15-16 CH_3	—	7.10		7.10
17eq-18	−70.057	—	−69.000	—
17ax-18	44.206	—	44.397	—
1′-2′	173.643	10.39	173.723	10.39
2′-3-	−180.000	11.60	−180.000	11.60
3′-4′	177.925	11.62	177.925	11.62
4′-5′	−175.603	10.92	−175.568	10.92
5′-6′ CH_3	—	7.10	—	7.10

Table 4. Calculated Dihedral Angles and Coupling Constants for Forocidins I

	(6) 9α-OH F I		(7) 9β-OH F I	
Proton	Calculated Dihedral Angle	Calculated J_{H-H}	Calculated Dihedral Angle	Calculated J_{H-H}
2β-3	−177.589	13.48	−177.065	13.43
2α-3	64.605	1.38	65.133	1.34
3-4	−52.874	−0.08	−52.062	−0.03
4-5	178.450	11.59	178.296	11.59
5-6	−67.324	0.50	−67.081	0.51
6-7β	−171.118	14.36	−173.054	14.54
6-7α	−56.074	3.82	−58.481	3.46
6-17eq	−64.451	2.78	−66.273	2.54
6-17ax	177.696	14.74	176.577	14.77
7β-8	−56.311	3.79	−58.586	3.44
7α-8	−170.085	14.96	−172.069	15.03
8-9	−50.796	3.61	73.683	1.39
8-19 CH_3	—	7.10		7.10
9-10	−169.163	—	71.230	—
10-11	−180.000	—	−180.000	—
11-12	−177.589	—	−178.483	—
12-13	177.762	—	177.762	—
13-14β	49.602	—	46.042	—
13-14α	167.278	—	163.603	—
14β-15	−55.189	3.06	−56.166	2.94
14α-15	−173.214	13.96	−174.145	13.99
15-16 CH_3		7.10		7.10
17eq-18	−70.018	—	−66.946	—
17ax-18	43.669	—	45.881	—
1′-2′	173.795	10.38	173.770	10.39
2′-3-	−180.000	11.60	−180.000	11.60
3′-4′	178.128	11.62	178.075	11.62
4′-5′	−175.694	10.93	−175.753	10.94
5′-6′ CH_3	—	7.10		7.10

Proton H-13 coupled to the doublet of doublets corresponding to the olefenic proton H-12 which in turn couples to the olefenic proton H-11. The doublet of doublets for proton H-11 showed cross-peaks into the olefenic proton H-10 which also appeared as a doublet of doublets. By virtue of the cross-peaks shown by each of the olefenic protons (H-10, H-11, H-12 and H-13) into the four carbon signals, the olefenic carbons (C-10, C-11, C-12 and C-13) were assigned.

The methine proton H-9 (position 9 is hydroxylated) shows a strong cross-peak to H-10 ($J_{9,10}$ = 9.7 Hz) and a weak one to H-8 (J, unresolved) in the COSY spectrum which was very similar to that observed in spiramycin I. The assignment of H-8 has been based on the weak cross-peaks into H-9, H-7b and a methyl group H-19. No cross-peak has been observed between the protons H-8 and H-7a. From the respective cross-peaks in the HETCOR spectrum, the carbon signals, C-8, C-9 and C-19 were identified. The methoxy methyl carbon C-20 showed a clear cross-peak in the HETCOR spectrum to a distinct singlet around 3.3 ppm for the methyl protons H-20. The signal at 174.0 ppm was assigned to the lactone carbonyl C-1.

Proton H-6 showed a moderate cross-peaks in the COSY spectrum to the methylen protons H-7a and H-7b, while no cross-peaks into the doublet for the methine proton H-5 were observed. The methylene proton H-7a could not be resolved completely, while H-7b appeared as doublet of doublet of doublets. The methylene protons H-7a and H-7b besides coupling to each other (geminal) could also couple to the protons H-6 and H-8. The calculated coupling constants for protons 7α (axial) and 7β (equitorial) obtained from the dihedral angles obtained for the minimized structure of 9α-OH forocidin I showed that each of the protons had a one small and two large J values (Table 4). Since proton H-7a was not resolved we were unable to characterize the stereochemistry of these protons.

Proton H-5 shows a cross-peak to the methine proton doublet H-4 which in turn couples into H-3. The methine H-3 was coupled to one of the methylene protons H-2a, more strongly than H-2b. Therefore, we have assigned the methine carbons C-3, C-4 and C-5. The methylene protons H-2a and H-2b besides showing geminal coupling (observed value for $J_{2a,2b}$ = 16.0 Hz) also coupled to H-3 (observed values for $J_{2a,3}$ = 11.0 Hz, $J_{2b,3}$ = 1.0 Hz). The calculated coupling constants for protons 2α (equitorial) and 2β (axial) are listed in Table 4. The results showed that coupling of H-2α to H-3 was small ($J_{2\alpha,3}$ = 1.4 Hz) while that of H-2β to H-3 was large ($J_{2\beta,3}$ = 13.5 Hz). Thus we can characterize H-2a as H-2β and H-2b as H-2α. Both pairs of methylene protons H-7a and H-7b, as well as H-2α and H-2β, show cross-peaks to C-7 and C-2 respectively in the HETCOR spectrum. The proton H-9 in (6) was assigned β stereochemistry (similar to spiramycin I) and the compound (6) as 9α-OH forocidin I. ^{1}H-NMR and ^{13}C-NMR assignments are listed in Tables 1 and 2 and the molecular modeling results in Table 4.

Epi-forocidin I [Compound IIB, (7)] (Fig. 3)

The ^{1}H-proton NMR spectrum of compound IIB (7) appeared similar to that of 9α-OH forocidin I (6) with regard to the loss of the two sugars and was identified as a 'forocidin I' analog since the hydroxyl group was at position C-9. All the other proton and carbon signals were assigned as in (6). The methine proton H-9 (position 9 is hydroxylated) showed strong cross-peaks to both H-10 ($J_{9,10}$ = 4.3 Hz) and H-8 (J, unresolved) in the COSY spectrum which was very different to that observed in the COSY spectrum of 9α-OH forocidin I or spiramycin I. For this isomer, proton H-9 was assigned α stereochemistry and the compound (7) as 9β-OH forocidin I. ^{1}H-NMR and ^{13}C-NMR assignments are listed in Tables 1 and 2 and the molecular modeling results in Table 4.

All the other proton and carbon signals were assigned in accordance with the spiramycin I structure. Molecular modeling studies using the X-ray data of demycarosyl leucomycin A_3 confirmed the stereochemistry of all the centers in IIA (6) and IIB (7) with the exception of the hydroxyl group at C-9. The compound was 'forocidin I-type' since the hydroxyl group was at position C-9. The methyl group H-19 along with the groups at carbons C-3, C-6 and C-15 have α (below the plane) stereochemistry. The proton H-9 coupled to H-8 in IIA (6) ($J_{8,9}$ = 3.4 Hz) and IIB (7) ($J_{8,9}$ = 1.0 Hz) and also to the olefinic proton H-10 which was larger in IIA (6) ($J_{10,9}$ = 9.7 Hz, which can also be cross-checked from the coupling patterns of H-10) than in IIB (7) ($J_{10,9}$ = 4.3 Hz, which can be obtained from the coupling patterns of H-10). The calculated coupling constant between protons H-9 and H-8 from the dihedral angles obtained for the minimized

structure of 9α-OH forocidin I was small ($J_{8,9\beta}$ = 3.6 Hz), while in the case of 9β-OH forocidin I was even smaller ($J_{8,9\alpha}$ = 1.4 Hz). The proton H-10 being olefinic, Karplus equation cannot calculate the coupling constants between protons H-9 and H-10. The proton H-9 in (6) was assigned β stereochemistry and the compound IIA was assigned as 9α-OH forocidin I. The proton H-9 in (7) was assigned α stereochemistry and the compound IIB was assigned as 9β-OH forocidin I (or epi-forocidin I).

Isoforocidin I [Compound IA, (4)] (Fig. 4)

The ^{1}H-proton NMR spectrum of compound IA (4) clearly indicated the loss of two sugars. The methylene protons H-14 which appeared as multiplets showed strong cross-peaks in the COSY spectrum to the downfield methine proton H-13 (~4.13 ppm, $J_{13,14}$ = 5.0, 13.9 Hz) which appeared as a doublet of doublet of doublets. This was different as compared to the forocidin I isomers where, proton H-13 appeared downfield in the olefinic region. The olefinic proton H-10 coupled to proton H-9 in the olefinic region (~6.08 ppm) which in turn showed a weak cross-peak into H-8 (J, unresolved) in the COSY spectrum. This difference in the cross-peaks indicated the presence of the hydroxyl group on carbon C-13 and the compound was classified as a 'isoforocidin I-type.' This indicated a rearrangement of the hydroxyl group from carbon C-9 to carbon C-13 and a subsequent migration of the conjugated diene system from C-10 through C-13 to C-9 through C-12. Therefore, an intramolecular allylic rearrangement had occurred in forocidin I yielding isoforocidin I as had been previously described in the hydrolysis of leucomycin A_3. All other protons were assigned in a fashion similar to the forocidin I compounds. For this isomer, proton H-13 was assigned β stereochemistry and the compound IA (4) as 13α-OH isoforocidin I. ^{1}H-NMR and ^{13}C-NMR assignments are listed in Tables 1 and 2 and the molecular modeling results in Table 3.

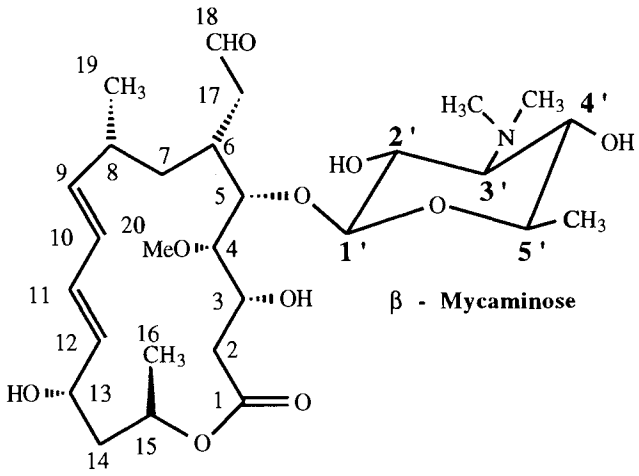

(4) Compound I A
13α-OH Isoforocidin I

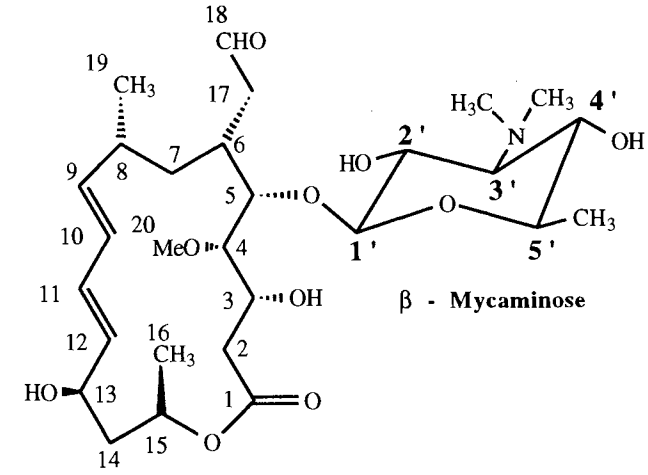

(5) Compound I B
13β-OH Isoforocidin I

Fig. 4. 13-OH Isoforocidins I.

Epi-isoforocidin I [Compound IB, (5)] (Fig. 4)

As with compound IA (4), the ^{1}H-NMR spectrum of compound IB (5) clearly indicated the loss of two sugars. In addition, the ^{1}H-NMR spectrum was very similar to that of the 13α-OH isoforocidin I (4). The methylene protons H-14 which appeared as multiplets showed strong cross-peaks in the COSY spectrum to the downfield methine proton H-13 (~3.79 ppm, $J_{13,14}$ = 0.9, 1.3 Hz) which appeared a doublet of doublet of doublets. This was clearly similar to 13 α-OH isoforocidin I (4) isomer. Here too proton H-9 (~6.08 ppm) in the olefenic region and an intramolecular allylic rearrangement had obviously occurred. All other protons were assigned in a fashion similar to the forocidin I-type compounds. For this isomer, proton H-13 was assigned α stereochemistry and the compound IB (5) as 13β-OH isoforocidin I. ^{1}H-NMR and ^{13}C-NMR assignments are listed in Tables 1 and 2 and the molecular modeling results in Table 3.

Molecular modeling studies confirmed the stereochemistry of all the centers in compounds IA (4) and IB (5) except for the hydroxyl group at C-13. Both compounds were 'isoforocidin I-type' since the hydroxyl group was at position C-13. The proton H-13 coupled to the methylene protons H-14 in IA (4) ($J_{13,14\alpha}$ = 13.9 Hz, $J_{13,14\beta}$ = 5.0 Hz) and IB (5) ($J_{13,14\alpha}$ = 0.9 Hz, $J_{13,14\beta}$ = 1.3 Hz) besides coupling to the olefinic proton H-12 (in IA (4) $J_{13,12}$ = 8.6 Hz, in IB (5) $J_{13,12}$ = 8.2 Hz). Coupling constants calculated from the dihedral angles obtained for the minimized structure of 13α-OH isoforocidin I indicated at least one small ($J_{13\beta,14\beta}$ = 3.1 Hz) and one large ($J_{13,14\alpha}$ = 13.6 Hz) coupling between H-13 and H-14 while in the case of 13β-OH isoforocidin I both the couplings for H-13 and the methylene protons were small ($J_{13,14\beta}$ = 2.7 Hz, $J_{13,14\alpha}$ = 0.03 Hz). The proton H-12 being olefinic, Karplus equation cannot calculate the coupling constants between protons H-13 and H-12. After comparing the observed and calculated values, the proton H-13 in (4) was assigned β stereochemistry and the compound as 13α-OH isoforocidin I while the proton H-13 in (5) was assigned α stereochemistry and the compound as 13β-OH isoforocidin I.

Currently there are few clinically suitable antibiotics available for the treatment of AIDS associated *Toxoplasma gondii* and *Cryptosporidium* infections. The anti-protozoal properties associated with the spiramycins may provide a foundation for the design of new and effective therapeutic agents to treat some of the most lethal opportunistic infections associated with AIDS. We are in the process of using both the spiramycins and the forocidins as models for determining structure activity relationships in hopes of providing information sufficient for the design of new 16-membered macrolide therapeutics.

ACKNOWLEDGMENTS

The authors express their deep appreciation to Dr. John K. Baker Alcon Laboratories Inc., Fort Worth, Texas, for providing valuable assistance in the structure elucidation aspects of this work. This work has been supported by grants from the ASP, AACP, Sigma Xi and the University of Mississippi.

REFERENCES

1. R. Corbaz, L. Ettlinger, E. Gaumann, W. Keller-Schierlien, F. Kradolfer, E. Kyburz, L. Neipp, V. Prelog, A. Wettstien and H. Zahner. Stoffwechselprodukte von Actinomyceten. Die Foromacidine A, B, C and D. *Helv. Chim. Acta.* 39, 304-317 (1956).
2. X. Saez-Lorens. Spiramycin for Treatment of *Cryptosporidium Enteritis. J. Infect. Dis.* 160, 342 (1989).
3. J. K. A. Beverly, A. P. Freeman, L. Henry and J. P. F. Whelan. Prevention of Pathological Changes in Experimental Congenital Toxoplasma Infections. *Lyon Med.* 230, 491-495 (1973).
4. K. Ramu, S. Shringarpure, S. Cooperwood, J. M. Beale and J. S. Williamson. ^{1}H-NMR and ^{13}C-NMR Spectral Assignments of Spiramycins I and III. *Pharm. Res.* 11, 458-465 (1994).
5. M. Hiramatsu, A. Furusaki, T. Noda, K. Naya, Y. Tomiie, I. Nitta, T. Watanabe, T. Take, J. Abe, S. Omura and T. Hata. The Crystal and Molecular Structure of Leucomycin A_3 Hydrobromide. *Bull. Chem. Soc.* 43, 1966-1975 (1970).
6. S. Omura, C. Kitao, H. Hamada and H. Ikeda. Bioconversion and Biosynthesis of 16-Membered Macrolide Antibiotics. X. Final Steps in Biosynthesis of Spiramycin, Using Enzyme Inhibitor: Cerulenin. *Chem. Pharm. Bull.* 27, 176-182 (1979).
7. O. W. Soerensen, S. Doenstrup, H. Bildsoee and H. J. Jakobsen. Suppression of J Cross-Talk in Subspectral Editing. The SEMUT GL Pulse Sequence. *J. Magn. Reson.* 55, 347-354 (1983).
8. A. Bax, R. Freeman and G. A. Morris. Correlation of Proton Chemical Shifts by Two-Dimensional Fourier Transform NMR. *J. Magn. Reson.* 42, 164-168 (1981).
9. A. Bax. Broadband Homonuclear Decoupling in Heteronuclear Shift Correlation NMR Spectroscopy. *J. Magn. Reson.* 53, 517-520 (1983).
10. W. J. Colucci, S. J. Jungk and R. D. Gandour. An Equation Utilizing Empirically Derived Substituent Constants for the Prediction of Vicinal Coupling Constants in Substituted Ethanes. *Magn. Reson. Chem.* 23, 335-343 (1985).
11. W. J. Colucci, R. D. Gandour and E. A. Mooberry. Conformational Analysis of Charged Flexible Molecules in Water by Application of a New Karplus Equation Combined with MM2 Computations: Conformations of Carnitine and Acetylcarnitine. *J. Am. Chem. Soc.* 108, 7141-7147 (1986).
12. H. Sano, M. Inoue, K. Yamashita, R. Okachi and S. Omura. Chemical Modifications of Spiramycins. Synthesis of the Acetal Derivatives of Neospiramycin I. *J. Antibiot.* 36, 1336-1344 (1983).
13. S. Omura, M. Katagiri, H. Ogura, T. Hata, M. Hiramatsu, T. Kimura, and K. Naya. The Chemistry of Leucomycins. II. Glycosidic Linkages of Mycaminose and Mycarose on Leucomycin A_3. *Chem. Pharm. Bull.* 16, 1402-1404 (1968).